

# LDC-VAE: A Latent Distribution Consistency Approach to Variational AutoEncoders

Xiaoyu Chen<sup>1</sup>, Chen Gong<sup>1</sup>, Qiang He<sup>1</sup>, Xinwen Hou<sup>1</sup>, and Yu Liu<sup>1</sup>

Institution of Automation, Chinese Academy of Science  
 {xiaoyu.chen, gongchen2020, heqiang2019, xinwen.hou,  
 yu.liu}@ia.ac.cn

**Abstract.** Variational autoencoders (VAEs), as an important aspect of generative models, have received a lot of research interests and reached many successful applications. However, it is always a challenge to achieve the consistency between the learned latent distribution and the prior latent distribution when optimizing the evidence lower bound (ELBO), and finally leads to an unsatisfactory performance in data generation. In this paper, we propose a latent distribution consistency approach to avoid such substantial inconsistency between the posterior and prior latent distributions in ELBO optimizing. We name our method as latent distribution consistency VAE (LDC-VAE). We achieve this purpose by assuming the real posterior distribution in latent space as a Gibbs form, and approximating it by using our encoder. However, there is no analytical solution for such Gibbs posterior in approximation, and traditional approximation ways are time consuming, such as using the iterative sampling-based MCMC. To address this problem, we use the Stein Variational Gradient Descent (SVGD) to approximate the Gibbs posterior. Meanwhile, we use the SVGD to train a sampler net which can obtain efficient samples from the Gibbs posterior. Comparative studies on the popular image generation datasets show that our method has achieved comparable or even better performance than several powerful improvements of VAEs.

**Keywords:** Variational AutoEncoder · Stein Variational Gradient Descent · Gibbs.

## 1 Introduction

In all the fields of machine learning, generative models play an important role, especially the unsupervised deep generative model, which has many successful applications in different fields, such as computer vision [4] and natural language processing [3]. With unsupervised deep generative model, one can build the model relate to the distribution on the observed data and generate more unseen data. Variational Autoencoders (VAEs) [17] and Generative Adversarial Networks (GANs) [11], as two most prominent unsupervised generative models serve the same purpose while different in their theories and implementations.

The VAEs view the data generation procedure as a random process which has a latent random variable, and utilize variational inference to train an encoder to approximate the distribution of the latent variable. Another decoder network is trained parallelly to simulate the data generation process which can generate new data when the

latent variable is given. While GANs directly model the data distribution using a generator network with the input from an arbitrary distribution, and apply a discriminator to evaluate the goodness-of-fit between the generated distribution and the real data distribution. Admittedly, the architecture of GANs seems to be plainer since it models the data distribution directly, but their training process is very unstable which often leads to convergence problems [1,12]. In the contrast, the VAEs can provide a relatively stable training process which attributes to its solid theoretical foundation.

However, the framework of the vanilla VAE has many flaws especially in the optimization of the evidence lower bound (ELBO), and finally hinders the performance of VAE in applications. First of all, the Gaussian assumption in the latent space gives the Kullback–Leibler (KL) divergence an analytical solution but also blocks the variational inference performance [5,18], since the encoder distribution is always relative with the input and hardly consistent with isotropic Gaussian.

Moreover, the trade-off between consistency in the latent space and the quality of the reconstruction always leads researchers in a dilemma. On the one hand, excessive consistency in latent space will cause the sample from the posterior irrelevant to the data, makes it difficult in training the decoder. On the other hand, giving the KL divergence a small coefficient indeed helps to retain more information about the input data, but it may destroy the consistency between the learned encoder distribution and the prior distribution (see Figure 1(a)). The samples from the inconsistent region, which between the encoder distribution (blue regions) and the prior (yellow region), will cause poor generation quality [6].

Furthermore, the isotropic Gaussian prior is hard to achieve in the latent space substantially [18,7,9], since the learned marginal distribution is a mixture Gaussian, and it is hard to get an isotropic Gaussian marginal distribution, even all the component posteriors are relatively close to isotropic Gaussian. Since the aforementioned problems of ELBO, many works focus on the improvement of it.

Different with most existing works which trying to make improvements on the ELBO, we take an alternative way to complete the variational inference that doesn't need to optimize the ELBO in VAEs. We model the gap between the real joint distribution  $p_\phi(x, z)$  and the approximate joint distribution  $q_\theta(x, z)$ , and optimize it by approximating the posterior  $p_\phi(z|x)$  directly rather than maximizing the ELBO (see Figure 1(b)). We achieve this purpose by assuming the  $p_\phi(z|x)$  in a Gibbs form. To complete efficient training, we use Stein Variational Gradient Descent (SVGD) [22] to get the gradient of the KL divergence between the learned posterior  $q_\theta(z|x)$  and the  $p_\phi(z|x)$ , which borrow the idea from Stein-VAE [27]. In the end, to address the problem which sampling from the Gibbs posterior needs the time expensively iterative method such as MCMC, we train a sampler net with SVGD to make efficient sampling from the Gibbs posterior.

In a word, our main contributions can be summarized as follows:

- Instead of optimizing the ELBO, we use a different way to complete the variational inference directly with our Gibbs posterior assumption. By doing this, we can optimize our LDC-VAE without the aforementioned ELBO problems.
- We utilize SVGD to train a sampler net, which can make efficient sampling from the Gibbs posterior rather than use a time-consuming sample method such as MCMC.

- The experiments show that our method has comparable or even better performance in all the compared improvements of VAEs.

The rest parts of our paper are organized as follows. In the related works, we give a brief conclusion of the works which analyzed and improved the VAEs. Then in the preliminaries, we retrospect the basic theory in VAEs and SVGD, which are fundamentals of our method. Our analysis and improvement of VAEs illustrate in the method part of this paper. In the end, we exhibit the performance of our work in both visualization form and statistics form.

## 2 Related Works

VAE [17] as a prominent generation model has many successful applications in a lot of machine learning fields, such as speech synthesis [25], text generation [31], transfer learning [32] and so on. Many works have been appealing in analyzing and improving its theoretical framework. Some works focus on making more complex and accurate approximation of the posterior of the latent space, such as using several samples to learn richer posterior [5], or adding a Inverse Autoregressive Flow (IAF) after the encoder [18].

Although these works can make more flexible and powerful approximation of the posterior in the latent space than the vanilla VAE, the optimization object of the encoder and decoder still remain its primitive problems. In fact, the KL divergence that forces every posterior close to the prior distribution is equivalent to making the posterior irrelevant to the input data [6,33]. However, the loss of the decoder needs the information related to the data to ensure the quality of the reconstruction [28]. To solve this problem and getting a relatively balance between the distribution consistency and reconstruction quality, researchers propose a series of methods, such as [3,15].

But even we apply all these methods to find an optimal ratio between the KL divergence and reconstruction loss, there is still a gap between the distribution of encoding space and the isotropic Gaussian prior [18,7]. This gap will lead some samples in latent space from the region that never be seen by the decoder in training, and finally cause a quality loss in generating new datas. Up to present, there are several ways to fix this issue, such as choose an autoregressive prior which obtained by using the IAF on the random noise [6]; apply a prior computing by a mixture posterior distribution condition on the learnable pseudo-inputs [29]. Also, it is an intuitive thinking that utilizing the Gaussian mixture model is a straightforward method, but it is not flexible enough comparing to the method above.

Our work is different with these methods that we do not make improvement on the ELBO. We bypass it using the Gibbs posterior assumption. It is worth to mention that there is also another way to avoid the ELBO in training VAEs which use a deterministic strategy such as RAE [9].

### 3 Preliminaries

#### 3.1 Variational AutoEncoder

VAEs model the data generation process as a random process with latent variable  $z$ , and try to inference its posterior distribution  $p_\phi(z|x)$ . While this posterior seems to be intractable, VAEs use an approximate distribution  $q_\theta(z|x)$  to approach it:

$$\text{KL} [q_\theta(z|x) \| p_\phi(z|x)] = \text{ELBO}(\theta, \phi, x) + \log p_\phi(x) \quad (1)$$

Since the  $\log p_\phi(x)$  is fixed when the dataset is given, minimizing the KL divergence on the LHS of Eq. (1) is equivalent to maximizing the ELBO:

$$\begin{aligned} \text{ELBO}(\theta, \phi, x) \\ = -\text{KL} [q_\theta(z|x) \| p_\phi(z)] + \mathbb{E}_{q_\theta(z|x)} [\log p_\phi(x|z)] \end{aligned} \quad (2)$$

To implement VAEs for data generation, the parametric forms of the three distribution in Eq. (2) must be specified. For simplicity, most of VAEs use the Gaussian form, in which the  $p_\phi(z) \sim \mathcal{N}(0, I)$ . The  $p_\phi(x|z)$  and  $q_\theta(z|x)$  are assumed to be the Gaussian distribution which parameter is determined by the output of the encoder and the decoder respectively:

$$z \sim q_\theta(z|x) = \mathcal{N}(z; \mu_\theta(x), \sigma_\theta^2(x)I) \quad (3)$$

$$x \sim p_\phi(x|z) = \mathcal{N}(x; \mu_\phi(z), \sigma_\phi^2(z)I) \quad (4)$$

By using the Gaussian assumption, the KL divergence term in Eq. (2) can be integrated analytically and calculate with the reparameterization trick. When the dimension of  $z$  is  $d$ , we have the  $\mathcal{L}_{KL}$  loss as follow:

$$\mathcal{L}_{KL} = \frac{1}{2} \sum_{j=1}^d \left[ \mu_\theta^j(x)^2 + \sigma_\theta^j(x)^2 - \log(\sigma_\theta^j(x)^2) - 1 \right] \quad (5)$$

For the reconstruction, calculating the value of the expectation of log-likelihood needs Monte Carlo method for approximation which will cost lots of computing resource for accuracy:

$$\mathbb{E}_{q_\theta(z|x)} [\log p_\phi(x|z)] \approx \frac{1}{M} \sum_{m=1}^M \log p_\phi(x|z_m) \quad (6)$$

But experiment in VAE [17] shows that the  $M$  can be set to 1 when the batch size of  $x$  is big enough (e.g. 100 in their paper). So for simplicity, set the  $\sigma_\phi^2(z)I = I$  and let  $M=1$ , we will have the reconstruction loss as:

$$\mathcal{L}_{REC} = \|x - \mu_\phi(z)\|^2 \quad (7)$$

### 3.2 Stein Variational Gradient Descent

In this section, we introduce the basic of SVGD, which is a nonparametric variational inference algorithm that integrates ideas from Stein method, kernel method and variational inference [21,22,23]. Recent years have witnessed the success of SVGD in machine learning [13,30,10].

**Assumption 1** We assume that  $q(x) : \mathcal{X} \subset \mathbb{R}^n$  is a continuously differentiable and positive p.d.f, and  $\Phi(x) : \mathbb{R}^n \rightarrow \mathbb{R}^n$  equals to  $[\phi_1(x), \dots, \phi_d(x)]^\top$ , which is a smooth vector function.

The SVGD aims to transport a set of initial particles  $\{x_i\}_{i=1}^n$  to approximate given target posterior distributions  $p(x)$ . The particles set  $\{x_i\}_{i=1}^n$  sampled from the distribution  $q(x)$ . SVGD achieves the approximation by leveraging efficient deterministic dynamics to iteratively updating the initial particles set  $\{x_i\}_{i=1}^n : x_i \leftarrow x_i + \epsilon \Phi^*(x_i)$ , where  $\epsilon$  is a small step size and  $\Phi^*$  is a function chosen to maximumly decrease the KL divergence. The  $\Phi^*$  is

$$\Phi^* = \arg \max_{\Phi \in \mathcal{B}} \lim_{\epsilon \rightarrow 0} \left\{ -\frac{d}{d\epsilon} \text{KL} (q_{[\epsilon \Phi]}(x) \| p(x)) \right\}, \quad (8)$$

where  $q_{[\epsilon \Phi]}$  is the particles distribution after the update leveraging  $x \leftarrow x + \epsilon \Phi(x)$ , and  $x \sim q(x)$ ;  $\mathcal{B}$  denotes the unit ball of reproducing kernel Hilbert space (RKHS):  $\mathcal{H}^d := \mathcal{H}_0 \times \mathcal{H}_0 \cdots \mathcal{H}_0$ , and  $\mathcal{B} = \{\Phi \in \mathcal{H}^d \mid \|\Phi\|_{\mathcal{H}^d} \leq 1\}$ . Fortunately, Liu & Wang prove that the result of Eq. (8) can be transformed to a linear function of  $\Phi$  [22],

$$\begin{aligned} \lim_{\epsilon \rightarrow 0} -\frac{d}{d\epsilon} \text{KL} (q_{[\epsilon \Phi]}(x) \| p(x)) &= \mathbb{E}_{x \sim q(x)} \left[ \text{trace} \left( \mathcal{T}_p^\top \Phi(x) \right) \right] \\ \mathcal{T}_p^\top \Phi(x) &= \nabla_x \log p(x)^\top \Phi(x) + \nabla_x^\top \Phi(x), \end{aligned} \quad (9)$$

where  $\mathcal{T}_p$  is called *Stein operator*. The  $\mathcal{T}_p$  and derivative  $\nabla_x$  is considered as  $\mathbb{R}^n$  column vectors, so the  $\mathcal{T}_p^\top \Phi(x)$  and  $\nabla_x^\top \Phi(x)$  can be viewed as inner products, e.g.,  $\nabla_x^\top \Phi(x) = \sum_{j=1}^d \nabla_{x^j} \phi_j(x) = \langle \nabla_x^\top, \Phi \rangle$ , where  $x^j$  and  $\phi_j$  are the  $j$ -th variable of vector  $x$  and  $\Phi$ . As the  $\Phi \in \mathcal{H}^d$ , the Eq. (9) equals to

$$\Phi_{q,p}^*(\cdot) = \mathbb{E}_{x \sim q(x)} [\mathcal{K}(x, \cdot) \nabla_x \log p(x) + \nabla_x \mathcal{K}(x, \cdot)], \quad (10)$$

where  $\mathcal{K}(x, \cdot)$  is a positive define kernel associated with RKHS  $\mathcal{H}^d$ . We obtain the Stein variational gradient to approximate  $\{x_i\}_{i=1}^n \sim q(x)$  to  $p(x)$ .

## 4 Method

Although the theoretical framework gives VAEs the merit of implementation convenience and training stability, the intrinsic drawbacks hinder VAEs to perform a satisfying generation result. Actually, as we mentioned before, the ELBO plays an important role in these defects.

In this section, we will introduce our method, which can be seen as an alternative version of VAEs without the ELBO.

#### 4.1 The LDC-VAE

To solve the inconsistency in  $\mathcal{L}_{KL}$  and the conflict between  $\mathcal{L}_{KL}$  and  $\mathcal{L}_{REC}$  in Eq. (2), we use a different formula that gets rid of the problems in the ELBO. We achieve this by minimizing the KL divergence between the joint distribution which is equivalent to minimize the KL divergence of two posterior distribution:

$$\begin{aligned}
& \text{KL} [q_\theta(x, z) \| p_\phi(x, z)] \\
&= \iint q_\theta(x, z) \log \frac{q_\theta(x, z)}{p_\phi(x, z)} dz dx \\
&= \iint q_\theta(x) q_\theta(z|x) \log \frac{q_\theta(x) q_\theta(z|x)}{p_\phi(x) p_\phi(z|x)} dz dx \\
&= \iint q_\theta(x) q_\theta(z|x) \log \frac{q_\theta(z|x)}{p_\phi(z|x)} dz dx \\
&= \mathbb{E}_{x \sim q_\theta(x)} [\text{KL} [q_\theta(z|x) \| p_\phi(z|x)]]
\end{aligned} \tag{11}$$

In the above equation, we use the assumption that  $p_\phi(x) = q_\theta(x)$ , since the  $x$  in the  $q_\theta(z|x)$  and the  $p_\phi(z|x)$  are both represent the data from the same dataset. The  $p_\phi(z|x)$  is the true posterior distribution of the latent variable  $z$ , and  $q_\theta(z|x)$  is our approximation posterior distribution which will be implemented by a deep neural network. And we set the KL loss in our model as follows:

$$\mathcal{L}_\theta = \text{KL} [q_\theta(z|x) \| p_\phi(z|x)] \tag{12}$$

For the true posterior  $p_\phi(z|x)$ , we assume it has a Gibbs form which is:

$$p_\phi(z|x) = \frac{1}{C} \exp \left\{ -\frac{\|x - D_\phi(z)\|^2}{\sigma^2} \right\} \tag{13}$$

The  $D_\phi(z)$  represents the reconstruction data. Although this formula doesn't seem to be a posterior distribution of  $z$  at the first glimpse, we must point out that for every given  $x$ , the Eq. (13) is a function of  $z$ , and can satisfied the equation  $\int p_\phi(z|x) dz = 1$  with an appropriate normalization factor  $C$ . Different with VAEs, we don't assume the form of  $q_\theta(z|x)$ , since it will cause the learned posterior lake of flexibility.

In the training, we use the encoder to approximate the proposed Gibbs posterior, and the learned latent distribution  $q_\theta(z) = \int q_\theta(z|x) q_\theta(x) dz = \int q_\theta(z|x) p_\phi(x) dx$  will finally consistent with the  $p_\phi(z) = \int p_\phi(z|x) p_\phi(x) dx$  if the training convergence properly. Since we use a posterior to approximate another posterior, the consistency in the formula form act as an insurance for the goodness-of-fit, helping our algorithm gets rid of the defects in the ELBO.

For the reconstruction loss, we minimize the  $\mathcal{L}_{REC} = \|x - D_\phi(z)\|^2$ . It is equivalent to maximizing the log-likelihood of the  $z$  from the Gibbs posterior when  $x$  has been observed, which is the second RHS term in the last equation in Eq. (14).

$$\begin{aligned}
& \mathbb{E}_{x \sim q_\theta(x)} [\text{KL} [q_\theta(z|x) \| p_\phi(z|x)]] \\
&= \mathbb{E}_{x \sim q_\theta(x)} \left[ \int q_\theta(z|x) \log \frac{q_\theta(z|x)}{p_\phi(z|x)} dz \right] \\
&= \mathbb{E}_{x \sim q_\theta(x), z \sim q_\theta(z|x)} [\log q_\theta(z|x)] \\
&\quad - \mathbb{E}_{x \sim q_\theta(x), z \sim q_\theta(z|x)} [\log p_\phi(z|x)]
\end{aligned} \tag{14}$$

The  $\mathcal{L}_\theta$  and  $\mathcal{L}_{REC}$  in our model can be interpreted as follows: minimizing the  $\mathcal{L}_{REC}$  loss will maximize the likelihood of  $z \sim p_\phi(z|x)$ , and minimizing the  $\mathcal{L}_\theta$  can make our encoder distribution consistent with  $p_\phi(z|x)$ .

Attribute to the Gibbs posterior which retains the information about  $x$ , the  $\mathcal{L}_\theta$  and  $\mathcal{L}_{REC}$  in our method are not mutually exclusive as what happened in the ELBO. Both the minimization of these two loss will lead to the minimization of the KL between the two joint distributions, so they can be optimized without conflict.

For the flexibility of the encoder distribution, we use a different implementation of encoder which doesn't apply the reparameterization trick. We input the noise from arbitrary distribution to the encoder and obtain the sample result directly (see Figure 1(b)). The output of our encoder is random even the input  $x$  is fixed:  $z = E_\theta(x, \epsilon_e) \sim q_\theta(z|x)$ . While in VAEs, the output of encoder represent the  $\mu_\theta(x)$  and  $\sigma_\theta^2(x)$  of the Gaussian distribution and will be fixed when the  $x$  is given. Due to this adaption, our encoder posterior distribution can approximate arbitrary distribution which depends on the parameter of the encoder.

**Algorithm 1** The LDC-VAE training process in iteration  $t$ **Input:**Batch of data  $x \sim p_\phi(x)$ ;Batch of noise from arbitrary distribution for the encoder  $\epsilon_e \sim f_e(\epsilon)$ ;Batch of noise from arbitrary distribution for the sampler net  $\epsilon_s \sim f_s(\epsilon)$ ;Model parameters of encoder and decoder  $E_\theta^{(t)}, D_\phi^{(t)}$ ;Model parameters of sampler net  $S_\omega^{(t)}$ **Output:** Updated parameters:  $E_\theta^{(t+1)}, D_\phi^{(t+1)}, S_\omega^{(t+1)}$ 

1: Obtain the output of encoder and decoder:

$$z_\theta = E_\theta^{(t)}(x, \epsilon_e), \hat{x} = D_\phi^{(t)}(z_\theta).$$

2: Compute the reconstruction loss:

$$\mathcal{L}_{REC} = MSE(x, \hat{x})$$

3: Calculate the gradient of encoder:

$$\Phi_\theta^*(z_\theta) = \frac{1}{n} \sum_{i=1}^n \mathcal{K}(z_i, z_\theta) \cdot \nabla_{z_i} \frac{\mathcal{L}_{REC}}{\sigma^2} + \nabla_{z_i} \mathcal{K}(z_i, z_\theta),$$

$$\frac{\partial \mathcal{L}_\theta}{\partial \theta} = \Phi_\theta^*(z_\theta) \cdot \frac{\partial z_\theta}{\partial \theta}$$

4: Update the parameter of encoder and decoder:

$$E_\theta^{(t+1)}, D_\phi^{(t+1)} = \text{Adam}(E_\theta^{(t)}, D_\phi^{(t)}, \frac{\partial \mathcal{L}_\theta}{\partial \theta}, \frac{\partial \mathcal{L}_{REC}}{\partial \phi})$$

5: Obtain the output of sampler net:

$$z_\omega = S_\omega^{(t)}(\epsilon_s)$$

6: Calculate the gradient of sampler net:

$$\Phi_\omega^*(z_\omega) = \frac{1}{n} \sum_{i=1}^n \mathcal{K}(z_i, z_\omega) \cdot \nabla_{z_i} \frac{\mathcal{L}_{REC}}{\sigma^2} + \nabla_{z_i} \mathcal{K}(z_i, z_\omega),$$

$$\frac{\partial \mathcal{L}_\omega}{\partial \omega} = \Phi_\omega^*(z_\omega) \cdot \frac{\partial z_\omega}{\partial \omega}$$

7: Update the parameter of sampler net:

$$S_\omega^{(t+1)} = \text{Adam}(S_\omega^{(t)}, \frac{\partial \mathcal{L}_\omega}{\partial \omega})$$

**4.2 Optimization with SVGD**

Although the  $\mathcal{L}_\theta = \text{KL}[q_\theta(z|x) \| p_\phi(z|x)]$  can be approximated using sampling-based method such as MCMC, it would be too slow and even difficult to convergence. In our implementation, we use the SVGD to approximate the gradient of  $\mathcal{L}_\theta$  w.r.t. the parameter  $\theta$ .

Specifically, we first compute the gradient of  $\mathcal{L}_\theta$  w.r.t. the  $z_\theta$ :

$$\begin{aligned} \Phi_\theta^*(z_\theta) &= \mathbb{E}_{z_i \sim q_\theta(z|x)} [\mathcal{K}(z_i, z_\theta) \nabla_{z_i} \log p_\phi(z|x) + \nabla_{z_i} \mathcal{K}(z_i, z_\theta)] \\ &= \frac{1}{n} \sum_{i=1}^n \left[ \mathcal{K}(z_i, z_\theta) \cdot \nabla_{z_i} \frac{\mathcal{L}_{REC}}{\sigma^2} + \nabla_{z_i} \mathcal{K}(z_i, z_\theta) \right] \end{aligned} \quad (15)$$

Then we set  $\Phi_\theta^*(z_\theta)$  act as a constant in the backpropagation and obtain the gradient of KL divergence w.r.t. to the parameter of encoder according to the chain rule:



Model	MNIST		CELEBA		CIFAR10	
	Rec	Sample	Rec	Sample	Rec	Sample
VAE	18.26	19.21	39.12	48.12	57.94	106.37
CV-VAE	15.15	33.79	40.41	48.87	37.74	94.75
WAE-MMD	10.03	20.42	<b>34.81</b>	53.67	35.97	117.44
2sAE	20.31	18.81	42.04	49.70	62.54	109.77
RAE-L2	10.53	8.69	43.52	47.97	32.24	<b>74.16</b>
RAE-SN	15.65	11.74	36.01	40.95	<b>27.61</b>	75.30
RAE-GP	14.04	11.54	39.71	45.63	32.17	76.33
LDC-VAE	<b>1.02</b>	<b>4.73</b>	34.82	<b>36.84</b>	49.18	101.24

**Table 1.** Quantitative evaluation of models using FID score. WAE-MMD denote the WAE with MMD loss. RAE-L2 denote the RAE with L2 regularization, GP denote the gradient penalty and SN denote the spectral normalization. All the sample FID of RAE models refers to generate new images using the ex-post density estimation (Gaussian Mixture Model).

$$\begin{aligned}
\frac{\partial \text{KL} [q_\theta(z|x) \| p_\phi(z|x)]}{\partial \theta} &= \frac{\partial \text{KL} [q_\theta(z|x) \| p_\phi(z|x)]}{\partial z_\theta} \frac{\partial z_\theta}{\partial \theta} \\
&= \Phi_\theta^*(z_\theta) \frac{\partial z_\theta}{\partial \theta}
\end{aligned} \tag{16}$$

Also, for the purpose that obtain efficient samples from the  $p_\phi(z|x)$ , we train a sampler net  $S_\omega(\epsilon_s)$  which maps an arbitrary distribution  $\epsilon_s \sim f_s(\epsilon)$  to the  $p_\phi(z|x)$  using SVGD. The gradient of KL divergence w.r.t to the parameter of sampler net has the same formula as the encoder.

The training procedure using SVGD is shown in Algorithm 1.

## 5 Experiment

To evaluate our method using empirical results, we design our experiment to test our model in two aspects: (i) the consistency of distribution in the latent space, (ii) sample and reconstruction quality. In this section, we will first specific our experiment details. Then, we provide the visualized evidence to show the inconsistency of VAE and how LDC-VAE achieves consistency in latent space. At the end of this section, we evaluate the image generation performance of our LDC-VAE in quantitive and qualitative ways.

### 5.1 Experimental Setup

In all the experiments on three datasets, we set  $f_e(\epsilon) = f_s(\epsilon) = \mathcal{N}(0, I)$  for the encoder and the sampler net. For the Gibbs posterior, we set the  $\sigma^2$  as the variance of  $\|X - D_\phi(z)\|$  in a batch. Due to the applying of the SVGD, the normalization factor C is trivial in our method. For the kernel function, we use the RBF kernel function  $\mathcal{K}(z, z_i) = \exp\left(-\frac{1}{h}\|z - z_i\|^2\right)$ . We set bandwidth  $h = \text{med}^2 / \log n$ , with med equal to the median of all the pairwise distance between  $z_i$  for all the  $n$  samples. According to [22], this setting

can balance the deviation from other  $z_j$  while computing the gradient of  $z_i$ . For the network architecture, we adapt the network in RAE [9]. We add a convolutional layer for the noise input in the encoder, and set our sampler net as same as the encoder in the RAE. For the convolution kernel size, we use the same kernel size in RAE, which has  $4 \times 4$  kernel size for MNIST and CIFAR-10, and  $5 \times 5$  for CELEBA. Also, we use a batchsize = 100 and [16, 64, 128]-dimensional latent space for MNIST, CELEBA and CIFAR10, which are identical to the hyperparameters in RAE. All the parameters of our networks are optimized using Adam [16].

## 5.2 Visualizing the Consistency of Distribution

The inconsistency between the encoder distribution and the prior is a vital defect of VAEs. This problem will cause some samples from the prior came from the region that never be seen by the decoder, and finally leads to the poor generation quality. To give clear visual evidence of this problem and prove our method indeed can alleviate this phenomenon, we train both the vanilla VAE and our model on MNIST with 16-dimensional latent space. To visualize the inconsistency problem of VAE, we compare 2000 test set samples from the encoder and 2000 samples from the prior. And to prove the consistency in latent space of our model, we compare the test set samples with samples from our sampler net. Both of the comparison are using scatter plot and project the 16-dimensional latent space to 2-dimensional using T-SNE [26].

As it can be seen in Figure 2(a), the marginal distribution  $q_\theta(z) = \int q_\theta(z|x)p_\phi(x)dx$  is not consistent well to the isotropic Gaussian and left a lot of uncovered regions. When generating new data, samples from these regions may have poor generation quality, since the decoder has never been trained to decode the latent variable from these regions. But with our model, due to the application of Gibbs distribution and our sampler net, the distributions in latent space can be much more consistent.

## 5.3 Quantitive and Qualitative Result for Image Generation

For quantitive evaluation, we report the FID score [14] on MNIST [20], CELEBA [24] and CIFAR10 [19] of our model. To make a fair comparison and prove the effectiveness of our method, we choose vanilla VAE and several improved versions which have been reported in the same network architecture. The baseline models include constant-variance VAE (CV-VAE) [2,8], Wasserstein VAE (WAE) [28], 2-stage VAE (2s-VAE) [7] and Regularized AutoEncoders (RAE) [9].

Specifically, The CV-VAE improved the vanilla VAE by fix the variance of  $q_\theta(z|x)$ , these leads to a stochasticity reduction for the encoder distribution. The WAE however, optimizing the VAE using two different regularizer, adversarial loss (WAE-GAN) or maximum mean discrepancy (WAE-MMD). We didn't choose the WAE-GAN for comparison, since it uses the adversarial loss which leads to an unstable training. The 2-stage VAE uses a two-stage remedy to learn a relatively precise latent space. And for RAE, they propose a deterministic training strategy which can bypass the optimization of ELBO. We compare with it since RAE can complete the same purpose as LDC-VAE do.

As can be seen in Table 1, attribute to the latent space consistency, our LDC-VAE outperform all the comparison models on MNIST, reducing the FID score from 10.03 to 1.02 and 8.69 to 4.73 for reconstruction and sample respectively. On CELEBA, we achieve superior sample performance, improving the FID score from 40.95 to 36.84. And for reconstruction, we achieve secondary performance which almost equal to the best (WAE-MMD). Also, on CIFAR10, our model obtain comparable performance with these advanced VAE models.

For qualitative result, we show the reconstruction results and the sample results on all the datasets in Figure 3, our model achieves good reconstruction and sample quality in MNIST and CELEBA.

## 6 Conclusion and Future Works

We propose the latent distribution consistent VAE (LDC-VAE), which serves as an alternative way to bypass the problems in ELBO. Firstly, we discuss the drawbacks of VAEs that are related to the ELBO, and introduce our LDC-VAE to avoid them. According to our derivation, the VAEs can be trained in a "posterior to posterior" strategy and lead to the consistent latent space theoretically. Also, we demonstrate the consistency of our model using scatter plot of latent space, and prove our LDC-VAE can achieve comparable or even better performance than several advanced VAEs. The future works will include the exploration of variant sampler net architecture which can obtain better sampling performance especially in high dimensional.

## References

1. Arjovsky, M., Chintala, S., Bottou, L.: Wasserstein generative adversarial networks. In: International conference on machine learning. pp. 214–223. PMLR (2017)
2. Ballé, J., Laparra, V., Simoncelli, E.P.: End-to-end optimized image compression. arXiv preprint arXiv:1611.01704 (2016)
3. Bowman, S.R., Vilnis, L., Vinyals, O., Dai, A.M., Jozefowicz, R., Bengio, S.: Generating sentences from a continuous space. arXiv preprint arXiv:1511.06349 (2015)
4. Brock, A., Donahue, J., Simonyan, K.: Large scale gan training for high fidelity natural image synthesis. arXiv preprint arXiv:1809.11096 (2018)
5. Burda, Y., Grosse, R., Salakhutdinov, R.: Importance weighted autoencoders. arXiv preprint arXiv:1509.00519 (2015)
6. Chen, X., Kingma, D.P., Salimans, T., Duan, Y., Dhariwal, P., Schulman, J., Sutskever, I., Abbeel, P.: Variational lossy autoencoder. arXiv preprint arXiv:1611.02731 (2016)
7. Dai, B., Wipf, D.: Diagnosing and enhancing vae models. arXiv preprint arXiv:1903.05789 (2019)
8. Ghosh, P., Losalka, A., Black, M.J.: Resisting adversarial attacks using gaussian mixture variational autoencoders. In: Proceedings of the AAAI Conference on Artificial Intelligence. vol. 33, pp. 541–548 (2019)
9. Ghosh, P., Sajjadi, M.S., Vergari, A., Black, M., Schölkopf, B.: From variational to deterministic autoencoders. arXiv preprint arXiv:1903.12436 (2019)
10. Gong, C., Bai, Y., Hou, X., Ji, X.: Stable training of bellman error in reinforcement learning. In: International Conference on Neural Information Processing. pp. 439–448. Springer (2020)

11. Goodfellow, I., Pouget-Abadie, J., Mirza, M., Xu, B., Warde-Farley, D., Ozair, S., Courville, A., Bengio, Y.: Generative adversarial nets. *Advances in neural information processing systems* **27** (2014)
12. Gulrajani, I., Ahmed, F., Arjovsky, M., Dumoulin, V., Courville, A.: Improved training of wasserstein gans. *arXiv preprint arXiv:1704.00028* (2017)
13. Haarnoja, T., Zhou, A., Abbeel, P., Levine, S.: Soft actor-critic: Off-policy maximum entropy deep reinforcement learning with a stochastic actor. In: *International conference on machine learning*. pp. 1861–1870. PMLR (2018)
14. Heusel, M., Ramsauer, H., Unterthiner, T., Nessler, B., Hochreiter, S.: Gans trained by a two time-scale update rule converge to a local nash equilibrium. *Advances in neural information processing systems* **30** (2017)
15. Higgins, I., Matthey, L., Pal, A., Burgess, C., Glorot, X., Botvinick, M., Mohamed, S., Lerchner, A.: beta-vae: Learning basic visual concepts with a constrained variational framework (2016)
16. Kingma, D.P., Ba, J.: Adam: A method for stochastic optimization. *arXiv preprint arXiv:1412.6980* (2014)
17. Kingma, D.P., Welling, M.: Auto-encoding variational bayes. *arXiv preprint arXiv:1312.6114* (2013)
18. Kingma, D.P., Salimans, T., Jozefowicz, R., Chen, X., Sutskever, I., Welling, M.: Improved variational inference with inverse autoregressive flow. *Advances in neural information processing systems* **29**, 4743–4751 (2016)
19. Krizhevsky, A., Hinton, G., et al.: Learning multiple layers of features from tiny images (2009)
20. LeCun, Y., Bottou, L., Bengio, Y., Haffner, P.: Gradient-based learning applied to document recognition. *Proceedings of the IEEE* **86**(11), 2278–2324 (1998)
21. Liu, Q., Lee, J., Jordan, M.: A kernelized stein discrepancy for goodness-of-fit tests. In: *International conference on machine learning*. pp. 276–284. PMLR (2016)
22. Liu, Q., Wang, D.: Stein variational gradient descent: A general purpose bayesian inference algorithm. *Advances in Neural Information Processing Systems* **29** (2016)
23. Liu, Q., Wang, D.: Stein variational gradient descent as moment matching. *arXiv preprint arXiv:1810.11693* (2018)
24. Liu, Z., Luo, P., Wang, X., Tang, X.: Deep learning face attributes in the wild. In: *Proceedings of International Conference on Computer Vision (ICCV)* (December 2015)
25. Luo, Y.J., Agres, K., Herremans, D.: Learning disentangled representations of timbre and pitch for musical instrument sounds using gaussian mixture variational autoencoders. *arXiv preprint arXiv:1906.08152* (2019)
26. Van der Maaten, L., Hinton, G.: Visualizing data using t-sne. *Journal of machine learning research* **9**(11) (2008)
27. Pu, Y., Gan, Z., Heno, R., Li, C., Han, S., Carin, L.: Vae learning via stein variational gradient descent. *arXiv preprint arXiv:1704.05155* (2017)
28. Tolstikhin, I., Bousquet, O., Gelly, S., Schoelkopf, B.: Wasserstein auto-encoders. *arXiv preprint arXiv:1711.01558* (2017)
29. Tomczak, J., Welling, M.: Vae with a vampprior. In: *International Conference on Artificial Intelligence and Statistics*. pp. 1214–1223. PMLR (2018)
30. Wang, D., Zeng, Z., Liu, Q.: Stein variational message passing for continuous graphical models. In: *International Conference on Machine Learning*. pp. 5219–5227. PMLR (2018)
31. Wang, T., Wan, X.: T-cvae: Transformer-based conditioned variational autoencoder for story completion. In: *IJCAI* (2019)
32. Zhang, Y.J., Pan, S., He, L., Ling, Z.H.: Learning latent representations for style control and transfer in end-to-end speech synthesis. In: *ICASSP 2019-2019 IEEE International Conference on Acoustics, Speech and Signal Processing (ICASSP)*. pp. 6945–6949. IEEE (2019)

33. Zhao, S., Song, J., Ermon, S.: Towards deeper understanding of variational autoencoding models. arXiv preprint arXiv:1702.08658 (2017)

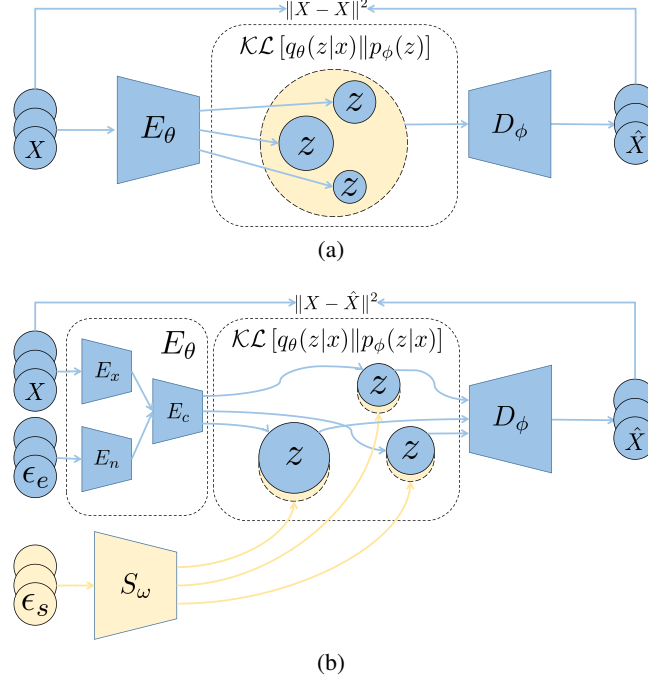


**Fig. 1.** The schematic diagram of vanilla VAE (Figure 1(a)) and our LDC-VAE (Figure 1(b)). In VAE, due to the substantial drawbacks in ELBO, the learned encoder distribution is always inconsistent with the prior, and leaves a lot of inconsistent regions (the uncovered yellow region in Figure 1(a)) that never be seen by the decoder while training. For LDC-VAE, since we use the encoder posterior to approximate the Gibbs posterior, we bypass the problems in ELBO and achieve more consistency in latent space. Since the reparameterization trick is not used in our encoder, we directly input the noise ( $\epsilon_e$  in Figure 1(b)) from arbitrary distribution to the encoder. We add a convolutional layer ( $E_n$ ) for the noise input, and leave the rest of the encoder ( $E_x$  and  $E_c$ ) identical with the RAE. Also, for efficient sampling, we train a sampler net ( $S_\omega$ ) parallelly which can map the noise from arbitrary distribution to the Gibbs posterior. The sampler net has identical architecture with the encoder in RAE.

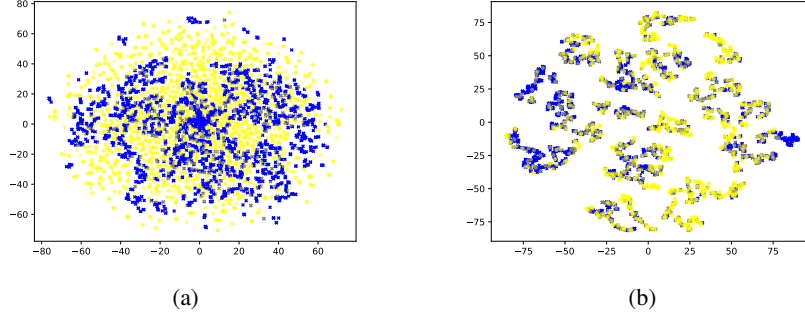


**Fig. 2.** Visualizing the latent space. The 16-dimensional samples are project to 2-dimensional using T-SNE. The blue points are encoder samples, while the yellow points come from the Gaussian prior in Figure 2(a) and Gibbs posterior in Figure 2(b). It is obvious that the inconsistency between the encoder distribution and isotropic Gaussian. And clearly, our method fix this problem to get a consistent latent space between the training and generation.

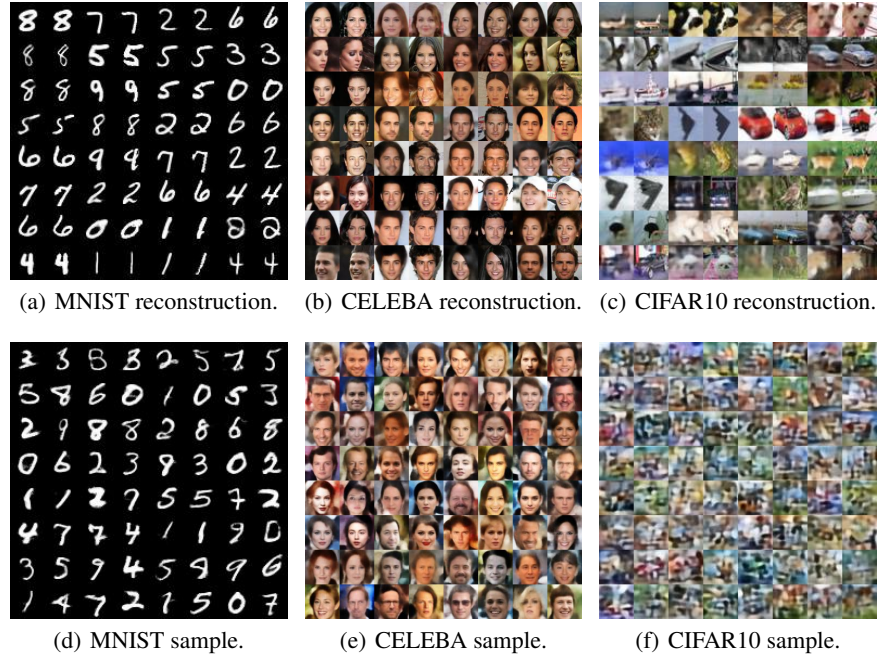


**Fig. 3.** The qualitative results for image reconstruction and generation on MNIST , CELEBA and CIFAR10. We set the odd columns for reconstruction images and even columns for original images for all the reconstruction result.